Princeton Plasma Physics Laboratory

PPPL-

PPPL-

PRINCETON PLASMA PHYSICS LABORATORY

Princeton Plasma Physics Laboratory
Report Disclaimers

PPPL Report Availability

Princeton Plasma Physics Laboratory:

http://www.pppl.gov/techreports.cfm

Office of Scientific and Technical Information (OSTI):

http://www.osti.gov/bridge

Related Links:

U.S. Department of Energy

Office of Scientific and Technical Information

Fusion Links

Plasma Modeling Results and Shape Control Improvements for NSTX

E. Kolemen 1), D. A. Gates 1), S. Gerhardt 1), R. Kaita 1), H. Kugel 1), D. Mueller 1), C. Rowley 2), V. Soukhanovskii 3)

1) Princeton Plasma Physics Laboratory, Princeton, NJ, USA
2) Princeton University, Princeton, NJ, USA
3) Lawrence Livermore National Laboratory, Livermore, CA, USA
E-mail contact of main author: ekolemen@pppl.gov

Abstract. New shape control implementations and dynamics studies on the National Spherical Torus eXperiment (NSTX) [8] are summarized. In particular, strike point position, X-point height and squareness control, and two new system-identification methods / control-tuning algorithms were put into operation. The PID controller for the strike point was tuned by analyzing the step response of the strike point position to the poloidal coil currents, employing the Ziegler-Nichols method. An offline system identification of the plasma response to the control inputs based on ARMAX [5] input-output models was implemented. With this tool, rough estimates of the improvements were realized and several control improvements were identified. An online automatic relay-feedback PID tuning algorithm, which has the advantage of tuning the controller in one shot, was implemented, thus optimizing the use of experimental time. Using these new capabilities, all four upper/lower/inner/outer strike points were simultaneous controlled and a combined X-point height, strike point radius control was implemented. The new and improved control with better accuracy and robustness enabled successful plasma operations with the liquid lithium divertor. Additionally this year, the first independent squareness control was developed. This will enable better optimization of the NSTX shape for stability and high performance in the future.

1. Introduction

Unlike general control systems, tokamaks have very fast time scales and large unmodeled disturbances, but limited and expensive experimental control-development time. The control tuning and the system-identification methods that fit these constraints are needed to operate current and future tokamaks. In this paper, new control implementations and dynamics studies on NSTX that help achieve these goals are summarized. Importantly, strike point position, X-point height, squareness control, and two new system-identification methods / control-tuning algorithms are implemented on a spherical tokamak for the first time. In this paper, we focus on the control improvements from 2010 and give an overview of results from 2009; for details, see Kolemen et al. [1].

In order to improve the performance of the plasma and better control the core plasma density, NSTX (R = 0.85 m, a < 0.67 m, R/a > 1.27) [8] has been investigating the use of lithium to condition the plasma-facing components. To reach this goal, NSTX has installed two evaporative lithium systems (LiThium EvaporatoR, or LiTER) to coat the graphite tiles that cover the inner walls [2, 3]. In 2010, the liquid lithium divertor was installed at NSTX in order to overcome the continuous increase in the core density during the shots. The liquid lithium divertor is a thick copper conic section with a thin layer of molten lithium on top, which is designed to absorb a significant particle flux (see Fig. 1). Because the lithium will continue reacting with hydrogen or deuterium until it is volumetrically converted to hydrides, the liquid lithium divertor is expected to provide better pumping than lithium coatings on carbon plasma facing components.

The particles that hit the NSTX wall dominantly follow the last closed flux surface and

thus land near the outer strike point, the location on the wall that has the same magnetic flux as the last closed flux surface. Employing the multi-fluid code UEDGE edge numerical plasma transport simulation code, Stotler et al. studied the effect of the reduced recycling that is provided by the liquid lithium divertor module [9]. These results show that density reduction depends on the proximity of the outer strike point to the liquid lithium divertor. To get better and more consistent density reduction, the strike point must be closely controlled. In addition, the strike point must avoid hitting the coaxial helicity injection gap [10] (see Fig. 1), since this may induce a disruption of the plasma. Finally, it is important to control the gap between the strike point and the liquid lithium divertor since the heat flux is very highly concentrated near the strike point, and this heat may be damaging to the liquid lithium divertor structure. Thus, in order to obtain better and more consistent density reduction and to avoid contact with the liquid lithium divertor and the coaxial helicity injection gap, the strike point position is of critical importance. With these motivations, we started the development and implementation of the strike point control algorithm.
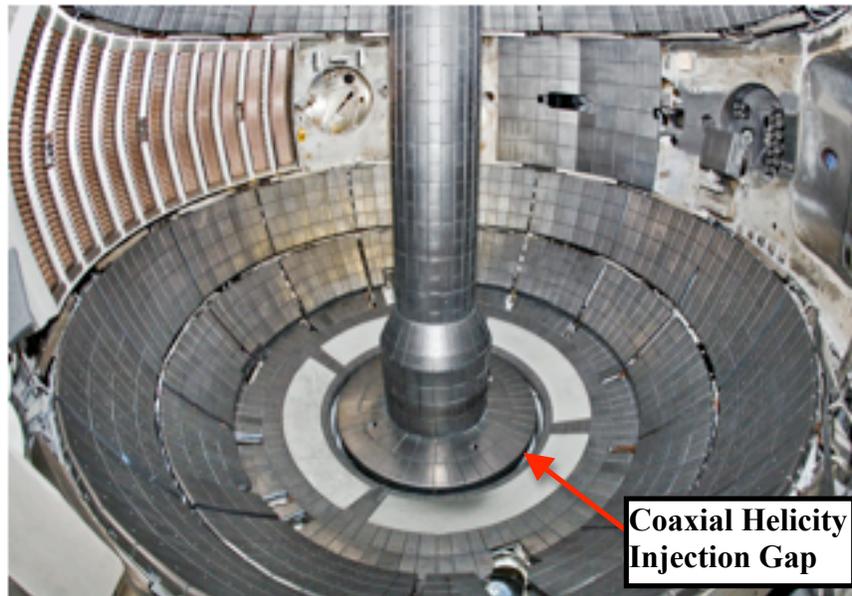
FIG. 1. Photo of the NSTX liquid lithium divertor installed near the inner edge of the outer divertor. Four 80° toroidal sections of 20 cm radial width separated by a row of graphite diagnostic tiles make up the liquid lithium divertor. Also shown in the figure is the coaxial helicity injection gap.

The previous controller needed further improvements before being part of the regular operations. There was excessive oscillation in the PF coils, the plasma was not sufficiently stable for controlled experiments, and many of the shots ended prematurely with disruptions. In order to better enable characterization of the liquid lithium divertor, improved strike point control was needed.

Plasma dynamics modeling was used as a basis for improved strike point control accuracy, since controller tuning via experiments can be time consuming. To maximize

the proportion of this process that is conducted offline, we implemented an offline system identification based on ARMAX (AutoRegressive Moving Average with eXogeneous inputs) input-output models [5]. With these models, rough estimates of the possible control improvements in accuracy and robustness were identified. These improvements were used as the initial guess for the experimental control fine-tuning. This offline algorithm implementation was used to develop a scenario consistent with the new requirements for operating the liquid lithium divertor, which include much tighter control of the strike points. The new algorithm has inner and outer strike point control for both upper and lower divertor, and optimized Proportional-Integral-Derivative (PID) gains for the combined inner and outer strike controllers.

An online automatic relay-feedback PID tuning algorithm was implemented for shape control within a real-time control system. This tuning method has the advantage of being able to tune the controller in one shot, which optimizes the use of experimental time. Also, due to its closed-loop nature, this online method is more robust to errors in plasma modeling. The experimental system identification and control tuning was improved via this method. A combined X-point height and strike point radius control was implemented with this tool and had the best performance in terms of robustness and accuracy.

The plasma boundary shape for NSTX has been studied extensively. Major shape parameters such as elongation and triangularity have been optimized for operations. However, the optimization of higher moments, such as squareness, of a tokamak cross-section can significantly enhance the stability to ideal magnetohydrodynamic ballooning and kink modes [13]. In order to further optimize the NSTX shape, a squareness control was implemented in the 2010 run year. This control can independently change the squareness without affecting other shape parameters. The preliminary testing of the control was performed.

In section 2 of this paper, strike point control improvements for the 2010 run are shown. The online automatic relay-feedback PID tuning algorithm and its implementation is shown in section 3. Finally, in section 4, the commissioning of the combined PF4 and PF5 coil operation and the new squareness control are summarized.

2. Improved Strike Point Control

In order to study the dynamics of the strike point, a proportional-integral control algorithm was implemented in the 2009 run to change the location of the strike point to the desired location, and to then stabilize it at the desired position. The polodial field (PF) coils that are most effective at changing the strike point location are PF1AL and PF2L, which are normally used to divert the plasma on NSTX (see Fig. 2. for coil locations). In order to measure the dynamics that are relevant to the strike point controller, the PF coil inputs for PF1AL and PF2L were changed in a stepwise fashion between various set-points, and the step response of the strike point position was obtained. Employing the analysis of the step response of the strike point position, the PID controller for the strike point was tuned, employing the Ziegler-Nichols method [1]. The controller was also

successfully employed to achieve the first "snowflake" divertor configuration in NSTX [4].
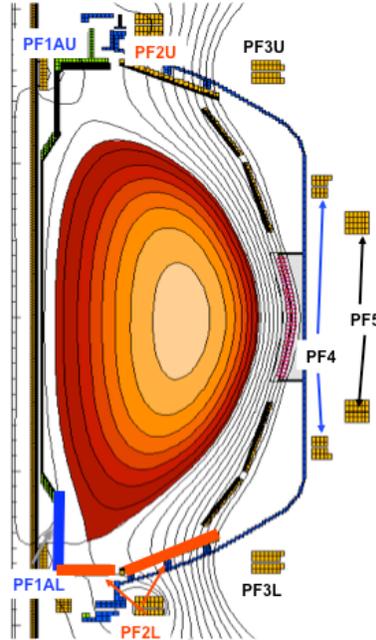
FIG. 2. NSTX Cross Section: PF2L controls the outer strike point in red segments, and PF1AL controls the inner strike point in the blue segment.

Improved strike point control was required to enable characterization of the liquid lithium divertor and prevent disruptions. To successfully measure the expected effect of the liquid lithium divertor, two major goals for the improvement were identified. The first one was to reduce the outer strike point control error RMS from 1.5-2 cm to 1 cm to enable the strike point to be kept on the liquid lithium divertor without drifting away and to minimize the measurement discrepancy due to the strike point oscillation. The second was to stabilize the vertical position of the plasma throughout the shot while the strike point control is turned on in order to create reproducible shots and narrow the difference between shots to the liquid lithium divertor only. In NSTX, the vertical position is characterized with Δr_{sep} parameter. Δr_{sep} is equal to the distance between the radial positions of the two points on the outer midplane that have the same flux as the upper and lower X-points respectively. Mathematically we can write this as $\Delta r_{sep}=[R(\psi(X_1)-R(\psi(X_2))]|_{Z=0,\ R>R0}$, where ψ is the toroidal flux at a given point, and the notation X_1 and X_2 are used for lower and upper X-points, respectively.

In the 2010 run, in order to reduce the RMS error of the outer strike point, plasma dynamics modeling was used as a basis for improved strike point control accuracy, since controller tuning via experiments can be time intensive. To maximize the proportion of this process that is conducted offline, the 2009 control experiment data was analyzed. Then, offline system identification was performed on the collected data to obtain a state-space realization. In the identified system, the PF coil voltages are the control input variables and the difference between the flux at the requested strike point location and the flux at the obtained strike point is the output variable. The flux difference was used as the

output variable since this parameter is used in the real feedback control algorithm. It is assumed that the system can be represented by a linear time-independent discrete input-output difference equation:

$$\mathbf{x}[k+1] = A\mathbf{x}[k] + Bu[k] + Gw[k]$$
$$y[k] = C\mathbf{x}[k] + v[k]$$

where k and $k+1$ are the indices of the discrete time step, u is the input variable (in our case, the voltage request sent to the power supplies), y is the output variable (in our case, the error between the requested and the achieved strike point), $\mathbf{x}$ is the unknown state vector (which in our case defines the combined effect of the internal dynamics of the plasma and the power supplies), $\mathbf{w}$ is the disturbance and v is the measurement noise. The aim is to find the minimal-state realization for the A, B and C matrices given only the measurements of y_k and u_k for a time interval. In our case, the state vector, $\mathbf{x}$, comprises the power supply, the inductance and resistance of the PF coil circuit, and the plasma boundary. However, since we do not specify the structure of this vector, each element of this vector does not have any specific physical meaning.

Linear system theory states that any state space model of the form given above can be rewritten as an innovations model (see [5] for details) for y(k) driven by a unique noise source e(k) as shown below.

$$\hat{\mathbf{x}}[k+1] = A'\hat{\mathbf{x}}(k) + B'u[k] + Ke[k]$$
$$y[k] = C'\hat{\mathbf{x}}[k] + e[k]$$

In this formulation the special form the matrices take are given as

$$
A' = \begin{bmatrix}
-a[1] & 1 & 0 & \cdots & \cdots & 0 \\
\vdots & 0 & \ddots & \ddots & & \vdots \\
\vdots & \vdots & \ddots & \ddots & \ddots & \vdots \\
\vdots & \vdots & & \ddots & \ddots & 0 \\
-a[d-1] & 0 & \cdots & \cdots & 0 & 1 \\
-a[d] & 0 & \cdots & \cdots & \cdots & 0
\end{bmatrix}, \
B' = \begin{bmatrix} b[1] \\ \vdots \\ \vdots \\ \vdots \\ \vdots \\ b[d] \end{bmatrix}, \
K = \begin{bmatrix} c[1]-a[1] \\ \vdots \\ \vdots \\ \vdots \\ \vdots \\ c[d]-a[d] \end{bmatrix}, \
C' = \begin{bmatrix} 1 \\ 0 \\ \vdots \\ \vdots \\ \vdots \\ 0 \end{bmatrix}^T .
$$

This can be rewritten as

$$
\begin{aligned}
y[k] &= -a[1]y[k-1] - \cdots - a[d]y[k-d] \\
&+ b[1]u[k-1] + \cdots + b[d]u[k-d] \\
&+ e[k] + c[1]e[k-1] + \cdots + c[d]e[k-d] .
\end{aligned}
$$

By defining the delay operator, q, as $q^j x$(k)=x(k+j), transfer functions G and H as

$$G = \frac{\sum\limits_{j=1}^{d} b[j]q^{-j}}{1 + \sum\limits_{j=1}^{d} a[j]q^{-j}}, \quad H = \frac{1 + \sum\limits_{j=1}^{d} c[j]q^{-j}}{1 + \sum\limits_{j=1}^{d} a[j]q^{-j}},$$

and $\boldsymbol{\theta} = $ [a[1], ..., a[d], b[1], ..., b[d], c[1], ...,c[d]], the state space system is equivalent to a standard ARMAX model of the form

$$y[k] = G[q, \boldsymbol{\theta}]u[k] + H[q, \boldsymbol{\theta}]e[k] .$$

Here $G[q,\boldsymbol{\theta}]$ is the transfer function that takes the input u to the output y and $H[q,\boldsymbol{\theta}]$ is the transfer function that describes the properties of the additive output noise model. Given an input-output recording of N points $(u[k], y[k])_{k=1,...,N}$ a minimization problem is solved in order to find the best estimate, $\hat{\boldsymbol{\theta}}$, of the parameters, $\boldsymbol{\theta}$, that define the system:

$$\hat{\boldsymbol{\theta}} = \arg\min_{\boldsymbol{\theta}} \sum_{k=1}^{N} e[k]^2.$$

Here, the best parameterization of the transfer function is selected to minimize the effect of noise on the system.

Time delays in the system have to be taken into account in order to avoid unphysically high dimensional models with bad match to the experiments. These delays were obtained from the experimental data and used as known variables in the system identification process. The delay in the system is between the output of the control and the action of the PF coils. Redefining the control input with a shift operator, $u[k] \equiv u[k-n]$, where n is the known delay in the system, we can keep the same formalism given above.

Collections of archived shots from last year's strike point control experiments were used to obtain the ARMAX model coefficients using MATLAB predictive error estimate algorithm [6]. These linear models consisting of the A, B and C matrices and the time delays in the system were obtained. An example of a PF2L to outer strike point error training set and the output of the model are shown in Fig. 3. The offline system identification gave close approximation of the experimental training data. The magnetic configurations used throughout this paper are determined by an EFIT code [16, 17]. The 'Basic' EFIT01 uses only the external magnetic measurements and simple models for plasma current and pressure. The 'Partial kinetic' EFIT02, when available, adds weak pressure constraints, allowing for edge currents and using higher order pressure and current approximations.

In order to validate the ARMAX models, they were checked against different data sets. An example of validation is shown in Fig. 4, where we compared the simulated model to the experimental step response. In the figure, the flux change is normalized by ΔIPF2L, the change in the PF2L coil current.
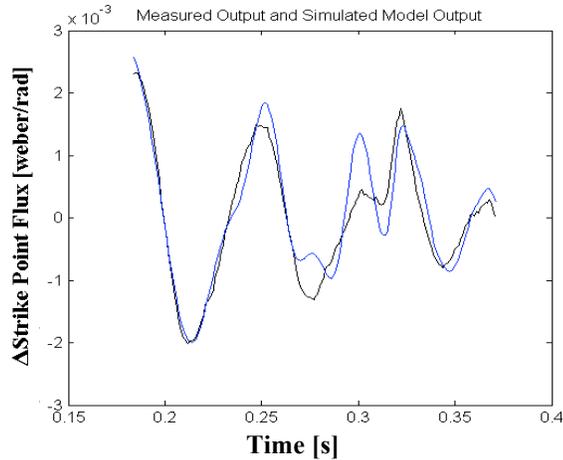
FIG. 3. Flux difference between the requested outer strike point location and the achieved location versus time. EFIT01 data for 133888 is shown in black and simulation of the ARMAX model is shown in blue.

Once the input-output systems were identified via ARMAX models, they were numerically simulated. The outputs of these simulations were employed to obtain the reaction curves, the same method that was used in the experimental tuning case. The rough estimates of the control improvements were obtained using the open loop PID tuning algorithms (see [1] for details). This included the retuning of the proportional and integral gains for inner and outer strike point, and estimates for a new PID control with derivative gain. These changes were implemented for both the inner and outer strike point.
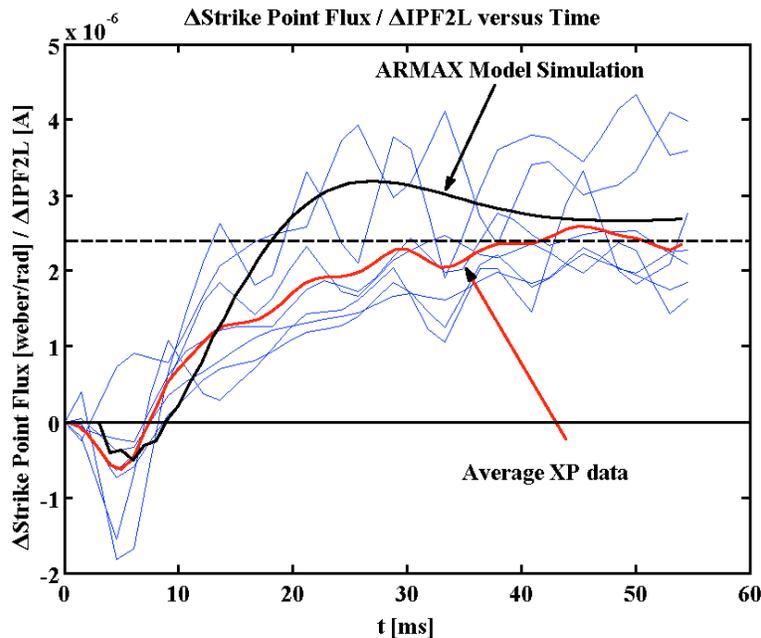

FIG. 4. Shown in black is the ARMAX model simulation and shown in blue are the experimental step responses from EFIT01. The average of the blue curves (Average XP data) is shown in red. For reference, the average experimental steady-state response is shown in a dashed line.

The control improvements led to reduced oscillations in the PF coils as shown in Fig. 5.a. This enabled stable plasma shots to have a longer flat-top. The stable plasma conditions allowed the strike point control capability to be used in regular physics experiments. When the lower PF coils are controlling the lower strike point location in feedback mode, they respond to the changes in the strike point locations. Since the upper PF coils are in feed-forward constant currents, this introduces an undesired vertical drift as the plasma evolves. In NSTX, this can be seen in the Δr_{sep} ramp as time progresses. For consistent experiments, it is important to stabilize this drift. Thus, upper strike point controllers were added. Copying the same controller designed for the lower coils to the upper ones, vertical symmetry was reintroduced to the system. Thus, lower and upper coils evolved together, avoiding the Δr_{sep} drift (see Fig. 5.b). Also, in order to reduce the bias error between the requested and achieved Δr_{sep}, integral gains were added to the PF3U/L controllers. These coils are not part of the strike point control but are used for vertical alignment. Taken together, these changes improved the control system substantially (see Fig. 6). This figure shows that we are able to closely track the outer strike point ramp request of 20 cm. Fine tuning of the control enabled the close tracking with the RMS errors to be kept below 1 mWb/rad with minimal oscillation. All four of the new control variables stay under simultaneous control throughout the shot. Noting that the outer gap is controlled via PF5 during these experiments, we achieved a tight control of the total plasma shape. This control became part of normal operations used in more than hundred shots in the 2010 run year.
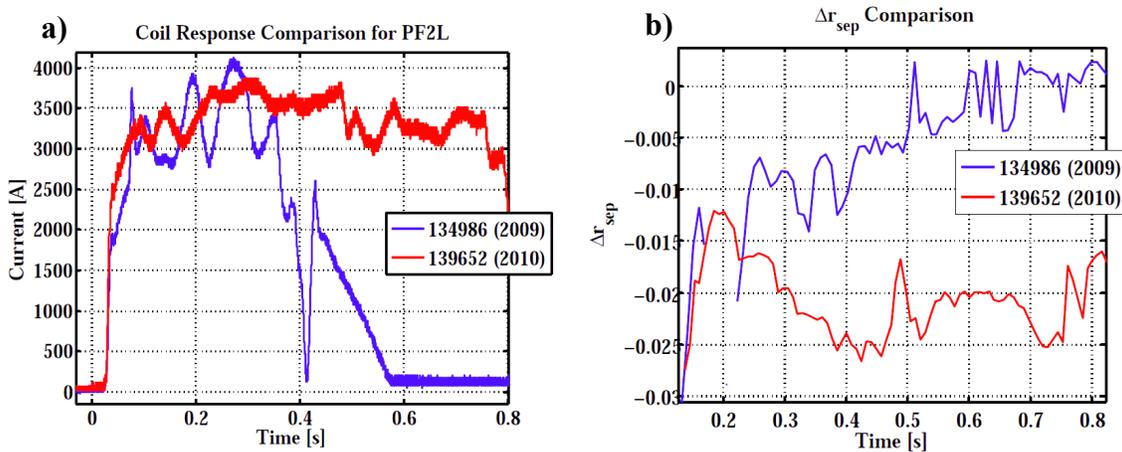

FIG. 5. Comparison of the Δr_{sep} and PF2L current evolutions from 2009 and 2010 (EFIT01).
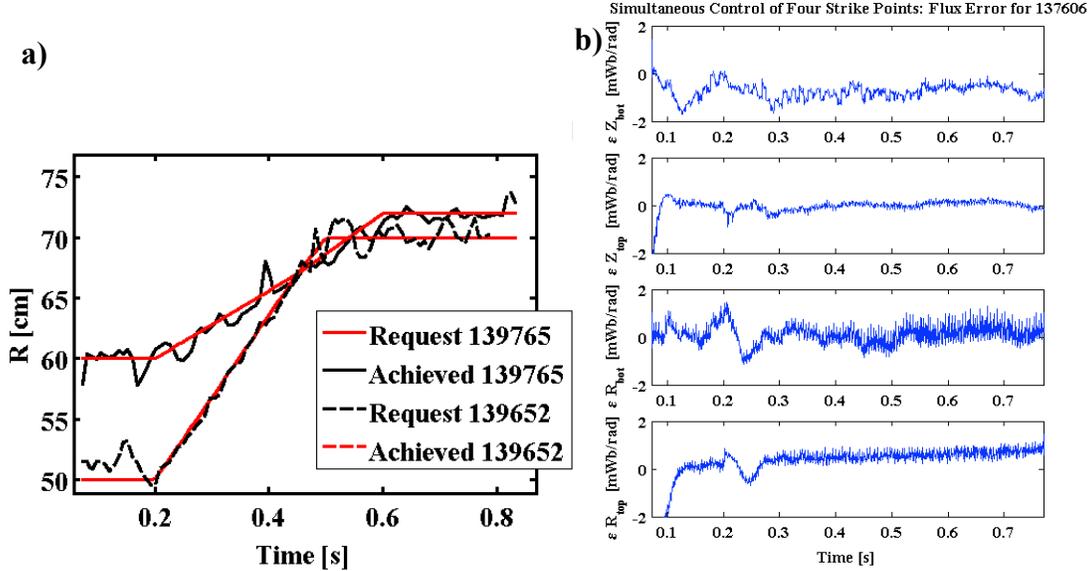
FIG. 6. (a) Two examples of lower outer strike point evolution with the improved control. (b) The performance of the simultaneous control of the four strike points (EFIT02).

3. Combined X-point Height and Outer Strike Point Control

After achieving a satisfactory control using the outer strike point controller in the 2009 strike point experiment, it was used for an experiment, which investigated an intermediate triangularity discharge with lithium plasma facing component coatings. While the controller kept the radial position of the outer strike point at the requested position, there were problems during the transient phase of the discharge. The equilibrium bifurcated to two solutions: the desired configuration with a medium X-point and the inner strike point on the vertical plate, and a configuration with a very low X-point and the inner strike point on the inner divertor plate. The solution oscillated between the two nearby equilibria. This led to the plasma scraping the divertor floor. To keep the plasma in the desired configuration and make it more stable, an inner strike point controller was added. While controlling the X-point height was the aim, we opted for the control of the inner strike point height instead. The reason for this was that PF1AL is very close to the inner strike point and thus that it was simple to control in a single-input-single-output (SISO) way via PF1AL without interfering with other control algorithms. While the goal of stabilizing the plasma around the correct equilibrium was mostly achieved during the flat top, during the first few-hundred-milliseconds transient phase, plasma touched the divertor lower tiles intermittently. Additionally, X-point height has a much greater effect on general plasma behavior than inner strike point location and is thus more beneficial as a control parameter. Thus, the experiment to control X-point height directly, instead of inner strike point height, was revisited in 2010.

The X-point position changes as a function of almost all the PF coils in the NSTX. Thus, it has much more complex dynamics than the inner strike point, and a multi-input-multi-output (MIMO) control would be the most appropriate for its control. Nevertheless, in order to simplify the first implementation of this control, it was kept as a SISO control. A future goal is to return to this topic to implement MIMO control. PF1AL is the closest

coil to the lower X-point and the most effective coil to control its height. As a result, it was used as the sole control input for X-point height control. In parallel with the PF1AL to X-point control, PF2L was used to control the outer strike point.

We have used a relay-feedback PID tuning algorithm to tune the PID controller used to control PF1AL and PF2L voltages. Previously, an open-loop system identification method was used, where a step change in the control parameter was introduced and the reaction curve of the process variable was observed. This procedure took many shots to identify the input-output pair and it was hard to isolate the exogenous effects during the uncontrolled time interval. In 2010, an online automatic relay-feedback PID tuning algorithm based on the Ziegler-Nichols method was implemented [11]. This tuning method has the advantage of enabling the controller to be tuned in one shot, which optimizes the use of experimental time. Also, this online method is more robust to errors in plasma modeling due to its closed-loop nature, thus improving the experimental system identification and optimal control tuning. This procedure is based on the idea of forcing the output to a specific oscillation via an on/off controller, also called a relay controller, whose dynamic behavior is shown in Fig. 7. Starting from its nominal bias value, the value of the voltage before the control turns on (20 Volts in the example case), the control action is increased by an amount denoted by h when the error is positive, and later decreased by −h when the error becomes negative. When choosing the h value, it is important to check that the induced oscillation is above the measurement noise and that the perturbation induced by the coils is not so large as to cause nonlinear effects on the system. Based on these insights, we chose the h value to be 250 Volts for the closed-loop system identification experiments. Since we are forcing the system in the closed-loop system identification, exogenous effects are isolated. Also, many cycles of oscillation in a single shot give us enough information to tune the control without repetition.
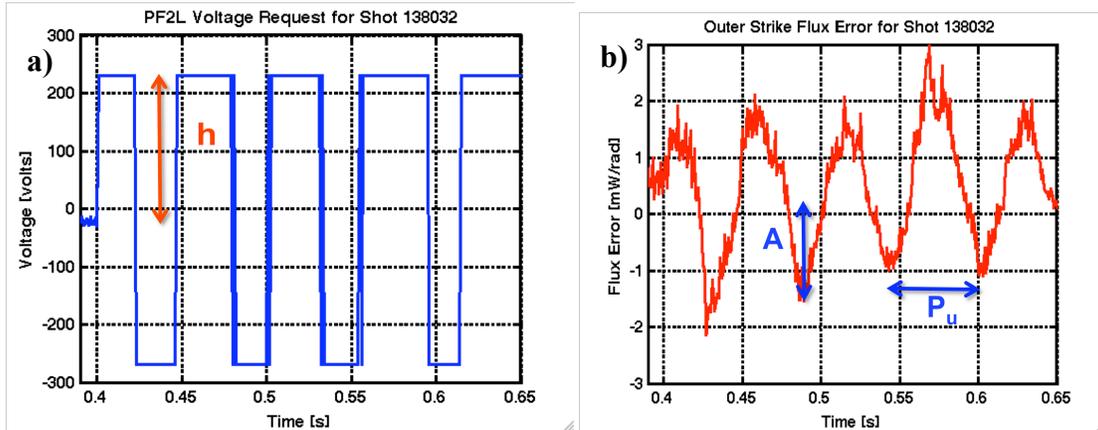

FIG. 7. A relay-feedback system identification example for NSTX used to tune to the PID controller for PF1AL and PF2L voltage
.

When the closed-loop plant response pattern is reached, the oscillation period (P_u) and the amplitude (A) of the plant response can be measured. From these values, the ultimate gain, $K_{cu} = 4h/(\pi A)$, can be calculated and used for the PID controller tuning, as shown in

Table I. Then, the voltage request, *V(t)*, is obtained from the PID formulation for given error, *e(t)*, as follows: $V(t) = K_{cu}(e(t) + \dfrac{1}{\tau_i}\int_0^t e(\zeta)d\zeta + \tau_d \dfrac{d}{dt}e(t))$.

TABLE I. THE ZIEGLER-NICHOLS TUNING METHOD

	K_c	τ_I	τ_D
P	$0.5K_{cu}$		
PI	$0.45K_{cu}$	$P_u/1.2$	
PID	$0.6K_{cu}$	$P_u/2$	$P_u/8$

The relay-feedback is used to tune the combined system consisting of the PF1AL, PF2L input to the X-point height, strike point radius output via the sequential SISO method [11]. In this method, first, the strike point radius control was tuned while X-point was not controlled. Second, X-point height control was tuned while the strike point used the control tuned in the previous step. Then, the strike point was tuned again while X-point height was controlled with the control tuned in the previous step. This procedure was repeated until the PID parameter designs between the steps were close to one another. Two iterations were used for the combined X-point height / strike point radius control. As shown in Fig. 8, the obtained control achieved <1 cm X-point height RMS error and <2 cm strike point radius RMS error after the initial transient. Note that, in this shot, the control is turned on at 165 ms, since real-time X-point calculations are not robust enough to be used before this point. For comparison, Fig. 9 shows the feed-forward strike point control just before this experiment under similar conditions. The feed-forward control where coil currents are manually adjusted to achieve strike point location was developed after many trials. The optimized feedback control enhances performance considerably. In normal operations, the radial position of the outer strike point is typically between 30 and 40 cm. The new combined controller enabled scanning the radial position of the outer strike point from 40 to 80 cm. Also, its robustness allowed pulses to last longer than the strike point only control or the hand tuned feed-forward control, as can be seen from Figures 5, 6, 8 and 9.

The developed feedback control algorithm was used for the liquid lithium divertor experiments to characterize its effect on particle absorption, which is expected to depend on the position of the outer strike point with respect to the liquid lithium divertor. Strike point drifts occurred during the feed-forward controlled operation, as shown in Fig. 9. Thus, if feed-forward control were used, it would not be possible to resolve the effect of the liquid lithium divertor from strike point drift. In the experiments, the outer strike point was placed on top of and at various distances from the liquid lithium divertor. In these scans, we used the combined controller to fix the X-point height. This was crucial to keep the plasma conditions as close to each other as possible between shots. Plasma density and various other parameters influenced by the liquid lithium divertor particle absorption were measured for these shots. The analyses of these measurements are continuing.
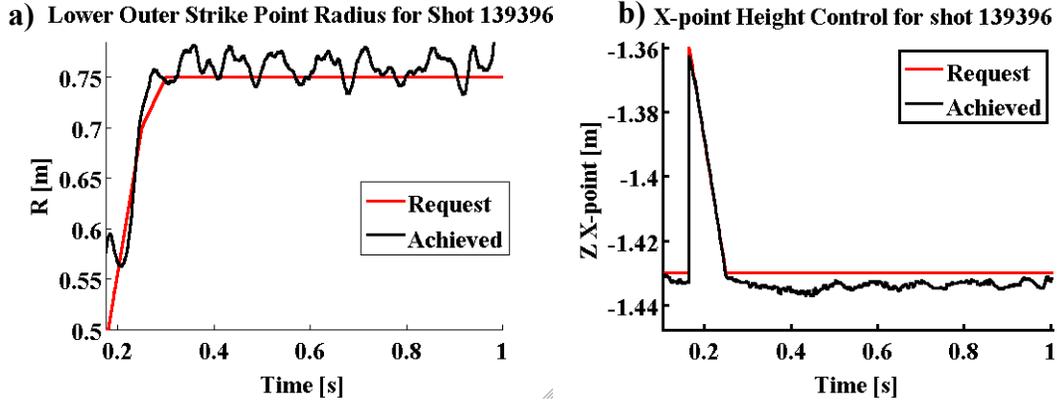
FIG. 8. Performance of the combined X-point height, strike point radius control (EFIT02).
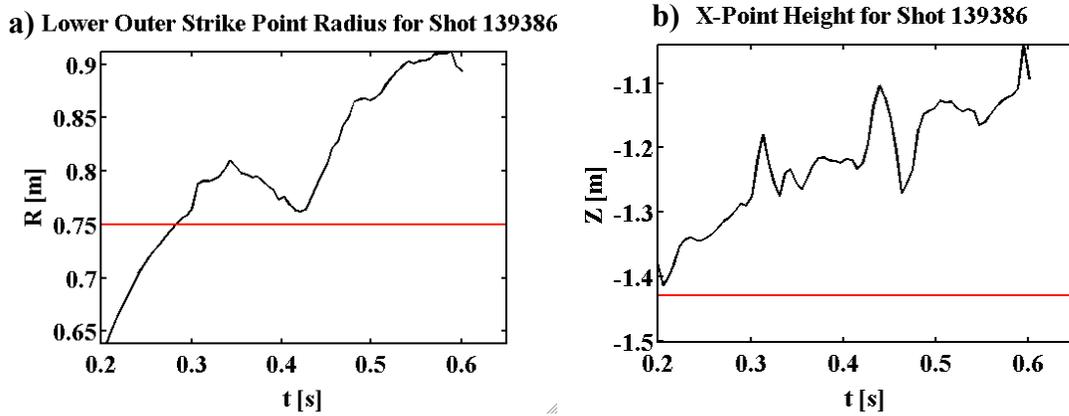

FIG. 9. Performance of the feed-forward (preprogrammed) strike point radius control shown in black. (Th red line is for reference purposes only)

4. The Combined PF4/PF5 Operation and Outer Squareness Control via PF4

NSTX will be upgraded with a bigger center stack and an additional neutral beam, which will allow a higher toroidal field (TF) $B_T = 0.55T \rightarrow 1T$, a plasma current of $I_P = 1MA \rightarrow 2MA$, a neutral beam injection heating power of $P_{NBI} = 5MW \rightarrow 10MW$, and a pulse length of $1s \rightarrow 5s$ [7]. The upgrade aims to attain 3-5 times lower collisionality with fully equilibrated profiles in full non-inductive operation. To achieve scenarios with high I_P and l_i, PF5 coil current alone will not be enough and PF4 and PF5 coils will have to operate simultaneously. The combined operation has hitherto not been part of normal operations.
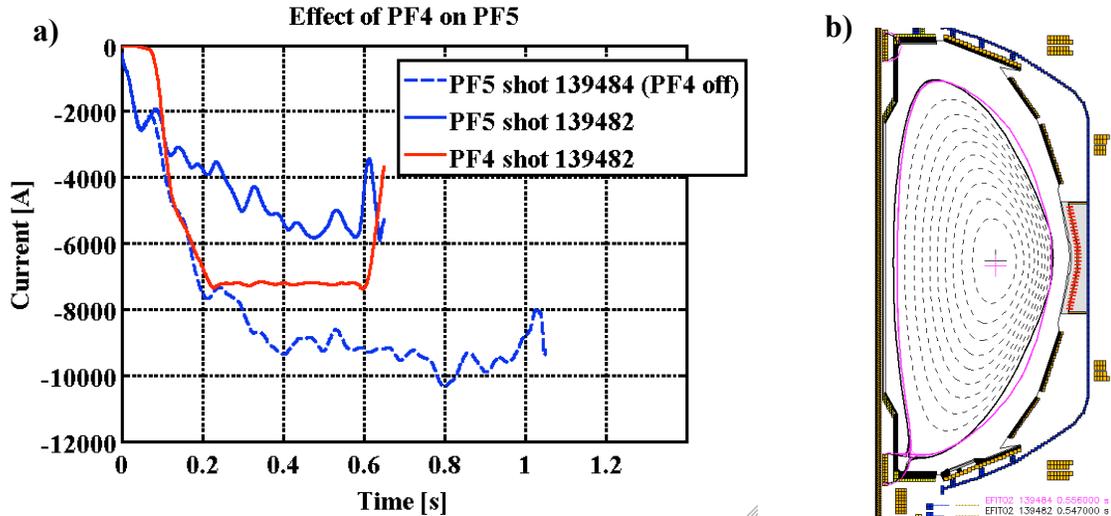
FIG. 10. (a) Coil currents for the PF5-only shot (139484) and the combined PF4/PF5 shot (139482). (b) The EFIT02 reconstruction of the boundary: the PF5 only shot (139484) is shown in magenta and the combined PF4/PF5 shot (139482) is shown in black.

In addition to its relevance to NSTX upgrade, the PF4 coil is useful for controlling the plasma squareness. The Spherical Tokamak devices all operate at high elongation in order to maximize the bootstrap fraction and cylindrical safety factor [15]. In addition, the location of the outer strike point during liquid lithium divertor operation has to be fixed. As a result, neither the plasma elongation nor the triangularity can be modified. An additional shape parameter that can help optimize plasma stability is the plasma ζ. Changing the ζ could modify the global stability, edge stability, or overall transport, as has been observed in DIII-D [13]. In NSTX, the coils that affect the ζ the most are the PF3 and PF4 coils. Since the upper and lower PF3 are used for vertical stability control, this leaves PF4 as the best candidate to vastly vary ζ with minimal side effect on the plasma.

In 2010, the simultaneous operation of these coils was commissioned. To prove the concept, a feed-forward PF4 input was implemented, keeping the PF5 coil for outer gap control and manually tuning the operation of other coils to achieve similar plasma parameters. Fig. 10.a shows a comparison of two shots, one with the PF4 coil turned off (the PF5 only shot) and another with the PF4 coil current set to -7 kA at flat-top. As seen from the experimental data on Fig. 10.b and simulation results from Fig. 11, obtained via ISOLVER (a predictive free-boundary auto-convergent axisymmetric equilibrium solver [14]), the introduction of PF4 along with PF5 changes the squareness of the plasma with minimal effect on the other shape parameters. Thus, PF4 enables independent control of the squareness, ζ, which is a shape parameter that defines how similar the boundary of the plasma is to a square, such that a triangle has ζ=0 and a rectangle has ζ=1.0. Early NSTX studies based on the ideal MHD analysis of the combined PF4/PF5 operation cases showed degradation of the stability due to the presence of the localized boundary indentations [12]. Experimental quantification of this effect will be studied as part of future work.
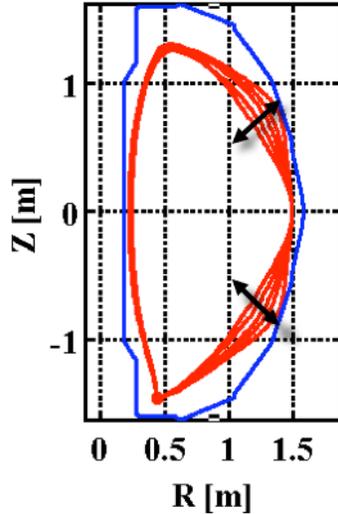
FIG. 11. The ISOLVER simulated effect of varying PF4 from -10 kA to +10 kA on the plasma boundary. The innermost boundary corresponds to -10 kA of PF4 current. Squareness increases as the PF4 current increases until it reaches the outermost boundary, which has +10 kA of PF4 current.

In order to control ζ, control of the plasma boundary via PF4 was employed. Two new control segments, starting from the plasma facing components at Z=±80 cm and R=140 cm and positioned perpendicular to the plasma boundary, were added in the control loop (approximate locations are shown with black lines in Fig. 11). In the control algorithm, the intersections of a given control segment with the real plasma boundary and the target plasma boundary that corresponds to the ζ request are computed. Then, the flux difference between these two points is obtained. The average of the flux differences at the upper and lower control segments, the segment error, was used to control the PF4 voltage request via a PID control algorithm. Initially, in order to facilitate a simple proof of concept control, we used a 40,000 Volts/(Wb/rad) proportional gain, leaving integral and derivative gains to be zero. Fig. 12 shows an example experiment with this ζ control. In this example, a difficult time-varying ζ target is requested to test the control performance. PF4 has a unidirectional power supply and thus cannot change sign within a shot. In this shot, it was arranged to have negative current only. Thus, PF4 cannot respond much to the positive change in ζ due to this zero current upper limit at the beginning phase, where PF3L and PF3U coils are doing most of the control. Starting at around 400 ms, the PF4 coil responds to a negative change in the ζ request. As seen in the figure, PF4 varies between zero and 2.5kA to achieve the request and stabilizes the segment error, which corresponds to the ζ error, around zero. The large swings in the coil current, starting at around 500 ms, are due to the untuned P-only control. Overreaction to the ζ request leads to excessive PF4 current and an overshoot of the request. As a result, the PF4 current is reduced to a very low level and a control-induced oscillation emerges. Tuning of the ζ control will be studied as a part of future work.
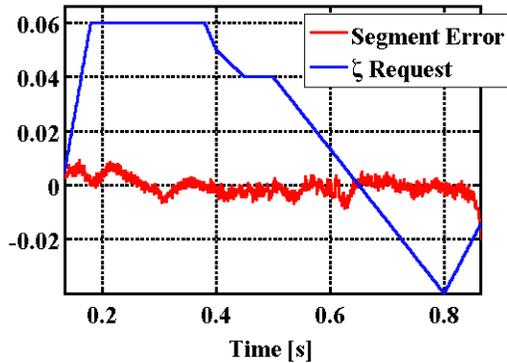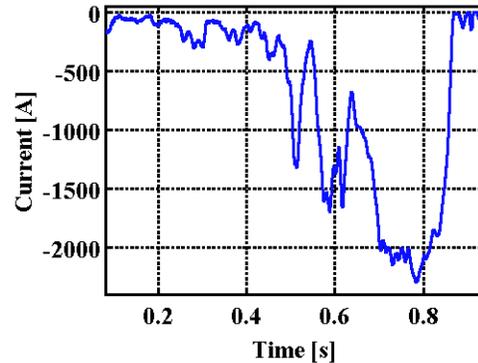
FIG. 12. Outer bottom ζ control via PF4. (a) The ζ request (unitless) and the segment error in Webers/rad. (b) The PF4 coil current.

5. Conclusion

In this year's NSTX operations, strike point position, X-point height and squareness control, and two new system-identification methods / control-tuning algorithms were put into operation. An offline system identification based on ARMAX models and an online automatic relay-feedback PID tuning algorithm were implemented. Employing these new capabilities, the strike point and X-point position controllers were tuned. The controllers were successfully implemented in liquid lithium divertor scenarios with simultaneous control of all four upper/lower/inner/outer strike points and with a combined X-point height, strike point radius control. Finally, an independent squareness control for NSTX was implemented for the first time, which will enable further optimization of the NSTX shape for higher performance and stability.

Acknowledgements

References

[1]   E. Kolemen et al., Nucl. Fusion, **50** 105010
[2]   H. Kugel et al., Fusion Engineering and Design, **84**, 1125 (2009)
[3]   H. Kugel et al., J. Nucl. Mater. 390–391 1000–4 (2009)
[4]   V. Soukhanovskii et al., Nucl. Fusion **51** 012001 (2011)
[5]   L. Ljung System Identification: Theory for the User, Prentice-Hall, NJ (1999)
[6]   MATLAB version 7.10.0. Natick, Massachusetts: The MathWorks Inc. (2010)
[7]   J. Menard et al., 37th EPS Conference on Plasma Physics, P2.106
[8]   M. Ono et al., Nucl. Fusion, **40** 557–61 (2000)
[9]   D. Stotler et al., Contrib. Plasma Phys. **50** 368–73 (2010)
[10]   R. Raman et al., Plasma Phys. Control. Fusion **43** 305–12 (2001)
[11]   C. Yu, Autotuning of PID Controllers: A Relay Feedback Approach, Springer-Verlag London Limited, Germany (2006)
[12]   F. Paoletti et al., Nucl. Fusion **42**, 418 (2002)
[13]   C. Holcomb et al., Phys. Plasmas **16**, 056116 (2009)

[14]   J. Huang et al., 47th Annual APS DPP Meeting, GP1 045 (2005)
[15]   J.E. Menard et al., Phys. Plasmas **11**, 639 (2004)
[16]   S.A. Sabbagh et al., Nucl. Fusion **41**, 1601 (2001)
[17]   S.A. Sabbagh et al., Nucl. Fusion **46**, 1 (2006)